JOURNAL OF CATALYSIS **163,** 148–157 (1996)
ARTICLE NO. 0314

Ammonia Synthesis Catalyzed by Ruthenium Supported on Basic Zeolites

Christopher T. Fishel,* Robert J. Davis,*,[1] and Juan M. Garces†

*Department of Chemical Engineering, University of Virginia, Charlottesville, Virginia 22903; and †Dow Chemical Company, Catalysis R&D, 1776 Building, Midland, Michigan 48674

Received March 21, 1996; revised June 7, 1996; accepted June 12, 1996

Ammonia synthesis was catalyzed by ruthenium metal clusters, promoted by alkali and alkaline earth elements, supported on zeolite X, magnesia, and pure silica MCM-41. At atmospheric total pressure and temperatures ranging from 623 to 723 K, the turnover frequencies of ammonia synthesis on Ru/KX varied significantly with Ru cluster size, demonstrating the known structure sensitivity of the reaction. Therefore, zeolite and magnesia catalysts were prepared with similar Ru cluster sizes, about 1 nm in diameter, in order to properly evaluate the effect of promoters. The same high degree of metal dispersion could not be obtained with Ru/MCM-41 catalysts. The turnover frequency for ammonia synthesis over Ru/CsX exceeded that over Ru/KX, consistent with the rank of promoter basicity. However, alkaline earth metals were more effective promoters than alkali metals for Ru supported on both zeolite X and MCM-41. Since alkaline earth metals are less basic, this promotional effect was unexpected. In addition, the turnover frequency for ammonia synthesis on Ru/BaX exceeded that of Ru/MgO, a nonzeolitic material. Pore volumes for Ru/BaX and Ru/KX measured by N_2 adsorption were essentially identical, suggesting that pore blockage by ions within the zeolites does not account for the differences in reaction rates. The kinetics of ammonia synthesis over ruthenium differed considerably from what has been reported for industrial iron catalysts. Most significantly, the order of reaction in H_2 was negative over Ru but is positive over Fe. A likely cause of this change in reaction order is that dissociated hydrogen atoms cover a greater fraction of the Ru clusters compared to Fe under reaction conditions.

INTRODUCTION

The standard industrial ammonia synthesis process using an iron-based catalyst requires temperatures between 673 and 973 K and pressures greater than 30,000 kPa, which results in an enormous energy demand for the process. Engineering advances during the past 40 years have reduced the energy required to produce 1 metric ton of NH_3 by a factor of three (1). Greater energy savings could be obtained by an improvement in catalytic activity that would allow for operation at lower temperatures and lower pressures. In the early 1970s, Ozaki and co-workers introduced a carbon-supported ruthenium catalyst promoted by alkali metal (Ru/AC–M, where AC is activated carbon and M is an alkali metal) (2, 3). At 523 K and 80 kPa, Ru/AC–K exhibited a 10-fold increase in the rate of NH_3 synthesis compared to a conventional promoted iron catalyst under similar conditions (2, 3). Since then, Ru/AC–K has been developed for industrial use (4).

Although activated carbon was the support for Ru in the pioneering work of Ozaki *et al.* (2, 3), Ru catalyzes the oxidation and methanation of carbon (5, 6). Thus, a more stable support is desirable. Aika and co-workers (7, 8) studied ruthenium supported on a series of oxides and found that the rate of ammonia synthesis increased as the intermediate Sanderson electronegativity of the support decreased.

The effects of different promoters were investigated by Murata and co-workers for ruthenium supported on Al_2O_3 (9, 10) and on MgO (11). On catalysts prepared using $RuCl_3$ as the source of ruthenium, one effect of alkali metal promoters is to enhance the reaction rate by removing chloride (9, 12). In addition, alkali metal was also found to be an effective promoter for chloride-free catalysts. The studies of Murata and co-workers demonstrated that enhancement of the reaction rate depends on a combination of the support and the promoter (10–12). Furthermore, their studies suggest that promotion of ruthenium supported on metal oxide may require contact between the promoter and ruthenium. On Ru/MgO, the effectiveness of the promoter was found to be inversely proportional to the electronegativity of the added metal. Also, for Ru/Cs–MgO, the reaction rate on a per gram basis reaches a plateau at a Cs/Ru ratio of 1(11). In contrast, on Ru/Al_2O_3, lanthanides were found to promote ammonia synthesis as effectively as cesium (10). However, for $Ru/Cs–Al_2O_3$, the reaction rate increased with the amount of promoter up to a Cs/Ru ratio of 10 (9, 10). These differences were ascribed to the proxim-

[1] To whom correspondence should be addressed.

0021-9517/96 $18.00

ity of the promoter to the Ru. Under reaction conditions, cesium probably exists as Cs_2O or CsOH, which may be attracted to Lewis acid sites on alumina so that the cesium spreads over the support. At a Cs/Ru ratio of 10, a nearly complete monolayer of CsOH is formed on the alumina (10). On the more basic MgO, CsOH is expected to remain near the Ru clusters (11). For Ru/Al_2O_3 promoted by lanthanides, the lanthanides are believed to migrate to the ruthenium–alumina boundary and undergo disproportionation over Ru to form lanthanide oxides (10). In each of these examples, contact between the ruthenium and the promoter was apparently required for effective promotion.

Explanations for the effects of the support and promoter on catalytic activity are a matter of contention. Aika *et al*. suggest that rate enhancement results from electronic promotion (8). Specifically, electrons are transferred from the support or promoter to the ruthenium metal, which lowers its ionization potential. The decreased ionization potential allows for electron transfer from the metal to the anti-bonding orbitals of the dinitrogen, reducing the activation energy for dissociative adsorption of N_2. The XPS spectra of Ru supported on alkaline-earth oxides showed binding energies shifted to lower values relative to ruthenium metal powder (8). In addition, the magnitude of the shift increased as the electronegativity of the support decreased, changing from 0.2 eV for Ru/BeO to 0.5 eV for Ru/MgO. Aika *et al*. attributed these binding energy shifts to electron donation from the support to the ruthenium metal (8). In contrast, Lee and Ponec discussed the effects of the support and promoters for alcohol formation from synthesis gas (CO and H_2) over supported Ru and argued against electron transfer effects for such materials (13). One objection was that any electron charge transferred to the ruthenium should remain localized at the metal–support or metal–promoter interface. Since the screening lengths in metals are on the order of a lattice constant (14), and since the ruthenium clusters in catalysts for both alcohol synthesis and ammonia synthesis are often greater than 5 nm in diameter (8, 13), the atoms at the metal–gas interface should remain essentially unaffected. In addition, Lang *et al*. describe a promotional effect of alkali metals adsorbed on catalyst surfaces in terms of an electrostatic interaction limited to the vicinity of the alkali (15). Some experimental evidence also suggests a lack of electron transfer from promoters to ruthenium. For example, the promoters typically exist as oxides or hydroxides under reaction conditions, and LEED analysis of Cs and O coadsorbed on a Ru(0001) surface indicated that the bond lengths are modified in a way consistent with efficient electron transfer from the cesium to the oxygen, rather than the ruthenium (16). Furthermore, proton NMR spectroscopy of H_2 chemisorbed on potassium-promoted Ru/SiO_2, with K/Ru ratios from 0 to 10, indicated no electron donation from K to Ru (17). Another possible method of promotion, similar to the mechanism favored by Strongin and Somorjai for promotion of iron by potassium (18, 19), is that the promoter lowers the energy of adsorption of ammonia on the Ru metal. Since the concentration of NH_3 on the surface decreases, more active sites remain available for dissociative adsorption of N_2. The principal evidence for this was provided by thermal desorption spectroscopy of NH_3 on Na-doped Ru(001) performed by Benndorf and Madey (20). As the Na coverage increased, NH_3 desorbed at lower temperatures, indicating that the NH_3 binding energy decreased with the addition of alkali (20).

Zeolites are of particular interest as supports, since the maximum metal particle sizes are limited to the sizes of the zeolite pores or cages. A review of platinum supported on zeolites suggests that such catalysts combine the intrinsic electronic effects of a small transition metal particle with electronic modifications resulting from the interaction of the metal particle with the strong ionic potential of the zeolite surface (21).

Ammonia synthesis catalyzed by ruthenium supported on alkali-metal-exchanged zeolites X and Y has been studied by Cisneros and Lunsford (22, 23). These materials were found to be catalytically active at atmospheric pressure over the temperature range 573–723 K. Even though the turnover frequency was lower on Ru/KX, their most active material, than the other nonzeolitic catalysts described in the literature, the fraction of ruthenium exposed was greater with the zeolite catalysts. Therefore, the Ru/zeolite systems compare more favorably on the basis of activity per total number of ruthenium atoms.

Cisneros and Lunsford found that the activity of zeolite-supported ruthenium was strongly dependent on the cations present in the zeolite (22, 23). For alkali-exchanged zeolite X, the turnover frequency increased in the order $Cs < Na < K$ (22, 23). This appears to contradict the results of Aika *et al*., who found cesium to be a more effective promoter than either potassium or sodium for both Ru/MgO (11) and Ru/Al_2O_3 (24). The effect of the alkali metal cation on the activity of ruthenium clusters in a zeolite is not straightforward, since many of the alkali metal cations are at ion-exchange sites at a distance from the ruthenium metal clusters. Also, the ruthenium is in contact with the oxygen atoms of the zeolite framework. Thus, the alkali may promote the ammonia synthesis reaction by modifying the electronic properties of the zeolite. Indeed, Cisneros and Lunsford concluded that the turnover frequency decreased as the partial oxygen charge of the zeolite support increased (22, 23).

In this paper, we describe the synthesis and reactivity of ruthenium clusters supported on various solid bases, particularly promoted zeolites and promoted magnesia, for the production of ammonia from dihydrogen and dinitrogen. The promoters examined are either alkali or alkaline-earth metals compounds.

EXPERIMENTAL METHODS

Catalyst Preparation

The starting material for the zeolite catalysts was high purity NaX from Union Carbide. Potassium X was prepared by ion exchange at room temperature of NaX three times with 1 *M* KNO_3. To produce a catalyst with a nominal metal loading of 2 wt% Ru, 15 g of NaX or KX were ion-exchanged with 0.936 g of $Ru(NH_3)_6Cl_3$ (Johnson Matthey) at 313 K. After ion exchange, the Ru/NaX and Ru/KX were each filtered and washed with a total of 6 liters of distilled deionized water to remove chloride. Silver nitrate tests of the filtrates confirmed the absence of chloride.

The Ru/KX was reduced before any futher ion exchanges were performed. First, the zeolite was dehydrated by heating *in vacuo* at 0.5 K min^{-1} to 723 K and holding at that temperature for 1 h. The material was cooled to room temperature and then reduced in flowing H_2. Dihydrogen was passed through a palladium purifier (Matheson 8371V) and then over the sample while the temperature was increased by 3 K min^{-1} to 723 K. The temperature was maintained at 723 K for 2 h, after which the sample was cooled to room temperature *in vacuo*. In previous studies, similar, evacuation and reduction of ruthenium exchanged into zeolites produced small metal clusters within the zeolite pores (22, 23, 25).

Reduced Ru/KX was used as the starting material to prepare Ru/CsX, Ru/BaX, and Ru/CaX. The zeolite was rehydrated by placing in a humid atmosphere overnight. The Ru/KX was then ion-exchanged three times at room temperature a 1 *M* solution of cesium acetate, barium acetate, or calcium acetate and filtered. Any acidic sites that may have been produced during the exchanges were neutralized by impregnation with 0.2 molal ($pH \geq 12$) aqueous solutions of KOH, CsOH, $Ba(OH)_2$, or $Ca(OH)_2$, as appropriate. The catalyst was then filtered, air dried, and sieved to 170 mesh.

In addition to the Ru/zeolite X catalysts synthesized in the lab, several have been provided and characterized by Dow Chemical Co. Elemental analyses of the catalysts made at the University of Virginia were performed by Galbraith Laboratories (Knoxville, TN).

To test the effects of support composition and structure on catalysis, MCM-41 and magnesia (Ube Industries) were also used as supports for ruthenium. MCM-41 is a mesoporous molecular sieve, with pore diameters ranging from 2 to 10 nm, depending on the synthesis technique (26), while zeolite X is microporous. The MCM-41 used here had a nominal pore diameter of 4 nm (27). Since pure silica MCM-41 and magnesia lack exchangeable ions like zeolite X, both the ruthenium and the promoter were introduced by impregnation. First, ruthenium was added by impregnation of the support with $Ru_3(CO)_{12}$ dissolved in THF. After being air dried at room temperature overnight, the material was heated *in vacuo* at 0.5 K min^{-1} to 723 K to decompose the carbonyl. The Ru catalyst was cooled to room temperature and then heated in flowing H_2 to 723 K and reduced for 2 h. Afterward, promoters were added by impregnation with aqueous cesium acetate or barium acetate. The acetate was decomposed by heating the material in flowing N_2 to 773 K.

Catalytic Rate Measurements

The system used to study ammonia synthesis consisted of a closed loop recirculation reactor with a pressure transducer. Prior to performing a catalytic study, the materials were dehydrated and reduced *in situ* as described previously. After reduction, the system was evacuated to $\leq 10^{-5}$ mbar and a 3:1 mixture of H_2 (Pd diffused) and N_2 (Roberts Oxygen, 99.999%, purified over MnO/SiO_2), initially at atmospheric pressure (100 ± 5kPa), was admitted to the system. As the reactants passed over the catalyst and circulated through the system at a rate of 0.037 liter (STP) s^{-1}, the ammonia produced was condensed in a liquid nitrogen trap, which minimized occurrence of the reverse NH_3 decomposition reaction. The reaction rate was monitored by measuring the pressure drop over time with a high-accuracy pressure gauge (MKS Baratron). The rates were measured at different temperatures in the range of 588–723 K to determine the apparent activation energy. The kinetics of the reaction were studied over selected catalysts by varying the N_2 and H_2 pressures; however, the order of reaction for NH_3 was determined by varying the gas flow rate in the reactor. In addition, ammonia synthesis was performed using D_2 instead of H_2 to determine if there is an isotope effect.

Gas Adsorption

The amount of H_2 chemisorbed on the ruthenium metal particles was measured by a conventional volumetric technique. The catalyst samples were dehydrated and reduced as was described previously. After reduction, the system was evacuated at 723 K for 1 h to remove chemisorbed H_2 and then cooled *in vacuo* to room temperature. A four-point H_2 chemisorption isotherm was then measured at room temperature. The intercept of the chemisorption isotherm, extrapolated to zero pressure, is the total amount of H_2 adsorbed. The dispersion of the ruthenium metal particles (the fraction of atoms in the particle at the surface) was calculated from the chemisorption isotherm by assuming that H_2 adsorbs dissociatively, with a H/Ru_{surf} ratio equal to 1. Dinitrogen adsorption isotherms were obtained on a Coulter Omnisorp 100CX instrument.

RESULTS

Elemental Analysis

The results from elemental analysis are shown in Table 1 for zeolite-supported catalysts and in Table 2 for magnesia-

TABLE 1

Elemental Analysis of Ruthenium on Molecular Sieve Supports

Catalyst	Ru Loading (wt%)	Support composition
Ru/KX	2.04	$K_{66.7}Na_{4.1}H_{7.5}Si_{113.7}Al_{78.3}O_{384}$
Ru/CsX	2.01	$Cs_{44.9}K_{15.5}Na_{9.8}H_{1.6}Si_{120.2}Al_{71.8}O_{384}$
Ru/CaX	2.21	$Ca_{55.2}K_{12.7}Si_{116.0}Al_{76.0}O_{384}$
Ru/BaX	2.05	$Ba_{41.8}K_{10.5}Si_{109.6}Al_{82.4}O_{384}$
Ru/BaX (II)	2.10	$Ba_{35.6}K_{8.5}Si_{116.1}Al_{75.9}O_{384}$
Ru/MCM-41	1.67	SiO_2
Ru/CsMCM-41	1.70	$Cs_{0.83}SiO_2$
Ru/BaMCM-41	1.26	$Ba_{0.65}SiO_2$

supported catalysts. Unit cell compositions of the zeolites are based on the assumption of 384 oxygen connected to Si and Al tetrahedra that match the molar ratio determined from elemental analysis. Protons were added to unit cell formulas to balance the framework charge when necessary. Ion exchange of K for Na was nearly complete in Ru/KX, and the exchanges of Ba or Ca for K were also essentially complete in Ru/BaX and Ru/CaX. In contrast, Cs exchange for K resulted in Cs occupying 62.5% of the available cation sites. Cisneros and Lunsford observed a lower exchange level of Cs into zeolite X (22, 23). The Ru/CsX in this work contained nearly twice as much cesium per unit cell as theirs (22, 23), and is in excellent agreement with the ion exchange isotherm (28, 29). The most likely reason for the level of cesium incorporation in zeolite X is the larger size of the Cs^+ ion (1.69 Å) compared to the Na^+ (0.95 Å), K^+ (1.33 Å), Ca^{+2}(0.99 Å), and Ba^{+2} (1.35 Å) ions (30).

The dispersions of Ru on the catalysts determined from H_2 chemisorption were used to estimate the cluster sizes that are summarized in Table 3. Ruthenium clusters supported on zeolite X have diameters of 1.0–1.3 nm, small enough to fit within the faujasite supercage. The Ru clusters on magnesia are of a similar small size. Since ammonia synthesis is known to be a structure sensitive reaction, it is important for comparison purposes that these samples have nearly the same Ru cluster size in order to separate structural effects from promoter and support effects. In contrast, the ruthenium particles supported on MCM-41 had dispersions of only 0.25–0.30. Attempts were made to synthesize Ru particles with smaller diameters on MCM-41, but without success. The exact reasons for this failure are unclear.

TABLE 2

Elemental Analysis of Ruthenium on Magnesia Supports

Catalyst	wt% Ruthenium	wt% Promoter
Ru/MgO	2.52	—
Ru/CsMgO	2.37	1.33
Ru/BaMgO	2.64	0.86

TABLE 3

Ruthenium Particle Sizes Determined by H_2 Chemisorption

Catalyst	Dispersion	Diameter (nm)
Ru/KX	0.93	1.0
Ru/CsX	0.72	1.3
Ru/CaX	0.83	1.1
Ru/BaX	0.92	1.0
Ru/BaX (II)	0.79	1.2
Ru/MgO	0.87	1.1
Ru/Cs-MgO	0.74	1.3
Ru/Ba-MgO	0.68	1.4
Ru/MCM-41	0.25	3.7
Ru/Cs-MCM-41	0.30	3.1
Ru/Ba-MCM-41	0.24	3.8

Interestingly, the pores of MCM-41 are nominally 4 nm in diameter (27), essentially the same size as the Ru clusters. Apparently, the metal particles grow to fit the space available in the pores of MCM-41.

The surface areas and micropore volumes of the zeolite X-based materials, both before and after being used as catalysts, are shown in Table 4. Following reaction, the maximum loss of micropore volume was approximately 6%. Similarly, Hathaway and Davis found that cesium-exchanged zeolite Y lost 4% of its crystallinity following calcination at 723 K (31). Surface areas and pore volumes after reaction for the MCM-41-based catalysts are listed in Table 5. The micropore volume for each of these catalysts was zero, as determined by the T-plot analysis method of Lippens and deBoer (32). This information, together with the high surface areas, indicates that the structural integrity of the MCM-41 support was maintained during impregnation and reaction.

Reaction Rates

The rates of ammonia synthesis over ruthenium clusters supported on alkali-exchanged zeolite X are shown in the Arrhenius-type plot in Fig. 1. The apparent activation energies, listed in Table 6, were all nearly 100 kJ mol^{-1}, which compares favorably with the results of previous studies

TABLE 4

Dinitrogen Physisorption Results for Ru Supported on Zeolite X

	Specific surface area ($m^2\ g^{-1}$)		Micropore volume ($cm^3\ g^{-1}$)	
Catalyst	Before reaction	After reaction	Before reaction	After reaction
Ru/KX	480	476	0.232	0.235
Ru/CsX	308	301	0.138	0.141
Ru/CaX	452	439	0.213	0.200
Ru/BaX	433	410	0.209	0.196

TABLE 5

Dinitrogen Physisorption Results for Ru Supported on MCM-41 after Reaction

Catalyst	Specific surface area ($m^2\ g^{-1}$)	Total pore volume ($cm^3\ g^{-1}$)
Ru/MCM-41	1058	1.015
Ru/CsMCM-41	623	0.417
Ru/BaMCM-41	713	0.596

TABLE 6

Ammonia Synthesis Catalyzed by Ruthenium Supported on Zeolite X

Catalyst	Ru dispersion	TOF at 623 K ($10^{-4}\ s^{-1}$)	E_a (kJ mol^{-1})
Ru/KX	0.93	1.91	106
Ru/CsX	0.72	4.85	91
Ru/CaX	0.83	14.9	106
Ru/BaX	0.92	14.1	115
Ru/BaX (II)	0.79	18.1	108

(3, 8, 22, 23). The turnover rate over Ru/CsX at 623 K was more than twice that over Ru/KX. This result differs with the findings of Cisneros and Lunsford that Ru/KX was the most active alkali-exchanged zeolite (22, 23). The reason for this difference is that a greater amount of cesium was incorporated into the catalyst in this work. This result verifies that Ru supported on zeolite X can be promoted by alkali metals in a way similar to Ru on nonzeolite supports. For example, cesium is a more effective promoter than potassium for both Ru/AC (3) and Ru/MgO (11).

The effects of impregnating the zeolites with hydroxide after ion-exchange are shown in Fig. 2. The NH_3 synthesis rates were 20–30% greater following hydroxide impregnation. This increase in reaction rate suggests that acid sites are neutralized by the hydroxide impregnation.

To study the effects of the size of the metal particles on catalytic activity, Ru/KX catalysts with dispersions of 0.93, 0.61, and 0.25 were prepared by varying the heating rate when the zeolite was dehydrated *in vacuo*. The cluster with a dispersion of 0.25 has a diameter of 3.7 nm, nearly three times the internal diameter of the zeolite supercage, and is presumably located on the external surface of the zeolite.

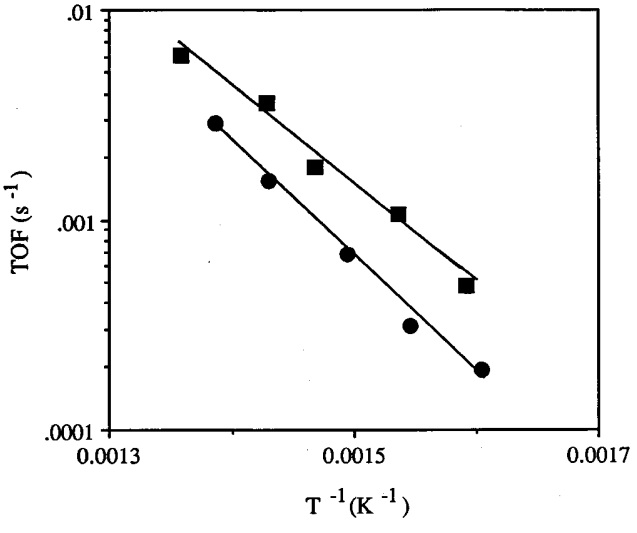

FIG. 1. Ammonia synthesis turnover frequencies over ruthenium supported on KX (circles) and CsX (squares).

As shown in Fig. 3, the turnover frequency increased as the dispersion decreased, which is consistent with earlier results (22, 23). Turnover frequencies over Ru/KX with a dispersion of 0.25 were greater than those over Ru/KX with a dispersion of 0.61 by a factor of 1.3–1.8 and greater than rates over Ru/KX with a dispersion of 0.93 by a factor of 3–4.

The rates of ammonia synthesis over ruthenium on alkaline-earth-exchanged zeolites are shown in Fig. 4 and Table 6. These catalysts are more active than alkali-exchanged zeolites, exceeding the turnover frequencies over Ru/CsX by a factor of 3–4. This is unexpected given earlier work that showed Ba to be a less effective promoter than Cs for Ru/MgO (11), and Ba and Cs to be about equally effective as promoters for Ru/AC (33). A second Ru/BaX catalyst was prepared and also used to catalyze ammonia synthesis. The results for this catalyst demonstrate that the successful promotion of Ru/X with Ba is reproducible.

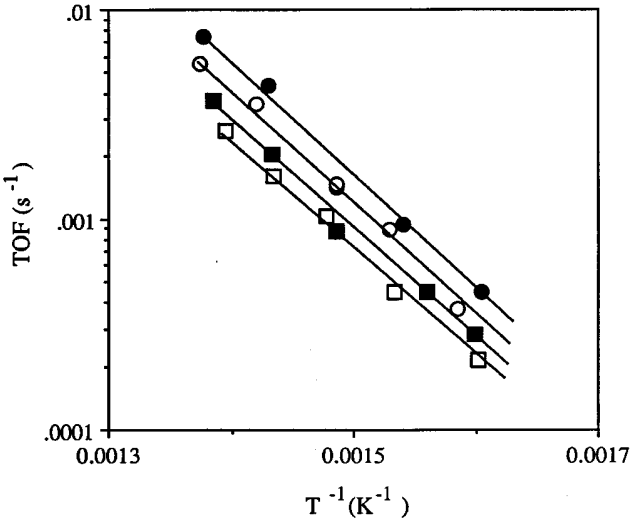

FIG. 2. Effects of hydroxide impregnation on ammonia synthesis rates over RuKX (squares) and Ru/CsX (circles) catalysts provided by Dow Chemical Co. Open symbols are samples without hydroxide treatment. Ruthenium loadings—Ru/KX, 1.70 wt%; Ru/KX + KOH, 1.36 wt%; Ru/CsX, 0.54 wt%; Ru/CsX + CsOH, 0.46 wt%. Zeolite compositions—Ru/KX, $K_{74.9}Na_{2.2}H_{22.6}Si_{92.3}Al_{99.7}O_{384}$; Ru/KX + KOH, $K_{78.6}Na_{2.7}H_{19.1}Si_{91.6}Al_{100.4}O_{384}$; Ru/CsX; $Cs_{49.9}Na_{42.5}H_{7.3}Si_{92.3}Al_{99.7}O_{384}$; Ru/CsX + CsOH, $Cs_{49.6}Na_{43.8}H_{6.1}Si_{92.5}Al_{99.5}O_{384}$.

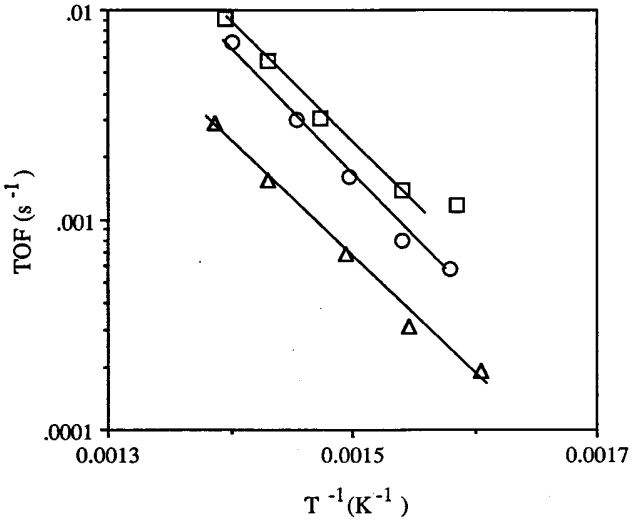

FIG. 3. Ammonia synthesis over Ru/KX catalysts of varying ruthenium dispersions. Dispersions are 0.25 (squares), 0.61 (circles), and 0.93 (triangles).

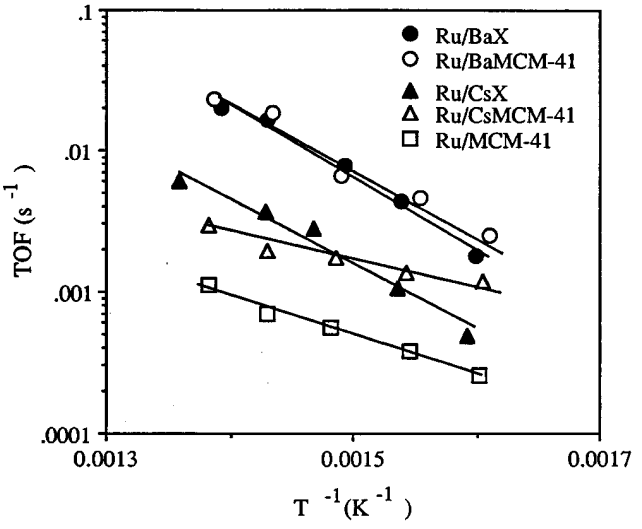

FIG. 5. Comparison of ammonia synthesis rates over ruthenium supported on MCM-41 and zeolite X.

The turnover frequencies measured over MCM-41-supported Ru catalysts are shown in Fig. 5. The unpromoted sample was the least active, whereas the Ba-promoted sample was the most active. Thus, the unexpected promotional effects of barium are not limited just to catalysts based on zeolite X. The analogous results for the alkali and alkaline-earth zeolite X catalysts are included in the figure. Even though the turnover frequencies of the Ba-promoted materials are similar, the Ru cluster size on MCM-41 is larger than on zeolite X. Therefore, the rate per total Ru in the sample is greater on the zeolite X material.

The reaction rates over promoted and unpromoted Ru on magnesia are shown in Table 7. The turnover frequencies over unpromoted Ru/MgO were similar to those over Ru/CsX and less than those over Ru/BaX. As shown in Table 7, the apparent activation energies over Ru/MgO and Ru/CsMgO were 15–25 kJ mol^{-1} less than the results of Aika *et al.* (11). The turnover frequencies for Ru/CsMgO at 588 K found by Aika *et al.* and found in this study are comparable, whereas the reaction rate over Ru/MgO in this work was four times greater than the rate for this material found by Aika *et al.* (11)

Addition of Ba to Ru/MgO caused the apparent activation energy to decrease markedly. Thus, although the turnover frequencies over Ru/BaMgO are less than those on Ru/CsMgO at high temperatures, the rates at 588 K are largest over Ru/BaMgO. A similarly low apparent activation energy for BaMgO can be calculated from the data of Aika *et al.* (11). Such large decreases in the apparent acti-

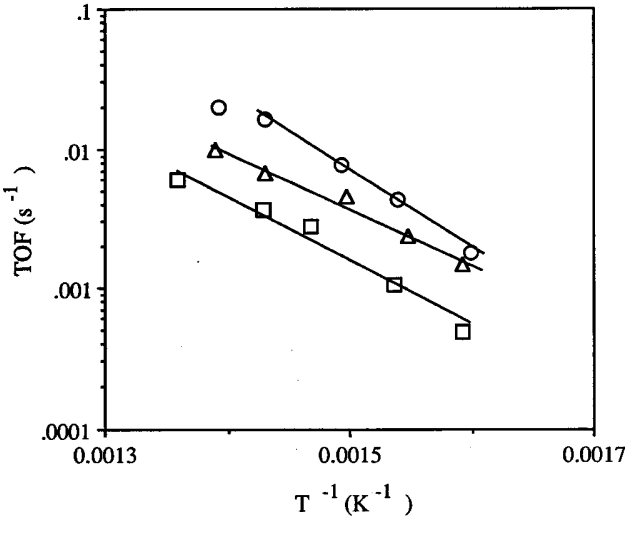

FIG. 4. Ammonia synthesis rates over ruthenium supported on BaX (circles), CaX (triangles), and CsX (squares).

TABLE 7

Ammonia Synthesis Catalyzed by Ruthenium Supported on Magnesia

Catalyst	Ru dispersion	Turnover frequency (10^{-4} s^{-1}) at 588 K	Turnover frequency (10^{-4} s^{-1}) at 623 K	E_a(kJ mol^{-1})
Ru/MgO	0.87	4.8	11.4	94
Ru/CsMgO	0.74	10.5	37.7	97
Ru/BaMgO	0.68	12.3	20.4	76
Ru/MgO[a]	0.67	1.24	—	125
Ru/CsMgO[a]	0.57	10.26	—	114
Ru/BaMgO[a]	—	(5.23)[b]	—	(67)[c]

[a] Results of Aika *et al.* (11); 2.0 wt% Ru; Cs/Ru ratio = 1.

[b] Calculated assuming that Ru/BaMgO had the same dispersion as Ru/CsMgO.

[c] Calculated from reaction rate data.

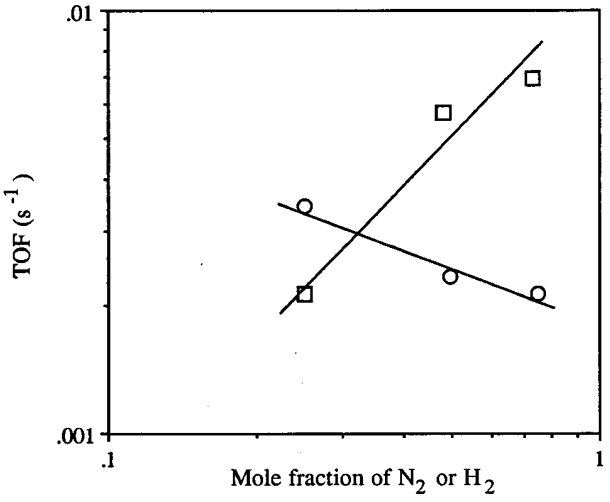

FIG. 6. Dependence of the ammonia synthesis rate on dinitrogen (squares) and dihydrogen (circles) mole fractions at 623 K. For variation of dihydrogen, the dinitrogen mole fraction was 0.25. For variation of dinitrogen, the dihydrogen mole fraction was 0.25.

vation energy apparently are not due entirely to the effects of barium, as indicated by the fact that the apparent activation energy of Ru/BaX is similar to the values for alkali-exchanged zeolite X. The change in apparent activation energy is presumably caused by the combined interactions of the promoter, the support, and the ruthenium metal. Although the apparent activation energies of the Ru/BaMgO in this study and in the work of Aika *et al.* were similar, the turnover frequencies differed by a factor of two (11). In our work, $Ru_3(CO)_{12}$ dissolved in tetrahydrofuran was used to impregnate magnesia with Ru. Previous studies by

TABLE 8

Orders of Reaction for Ammonia Synthesis over Ruthenium Catalysts

Catalyst	Reaction orders		
	N_2	H_2	NH_3
Ru/BaX	1.0	−0.46	−0.42
Ru/SiO_2[a]	1.1	−0.48	−0.56
$Ru/K\text{-}SiO_2$[a]	0.7	−1.0	−0.13

[a] From Nwalor and Goodwin (35).

Aika *et al.* have demonstrated that differences in the precursors for the promoter and the ruthenium can affect the rate of ammonia synthesis over Ru/CsMgO by more than a factor of two (8).

Kinetics

The variations of the rate of ammonia synthesis over Ru/BaX with changing N_2 and H_2 pressures are shown in Fig. 6. The changes in the reaction rate as the flow rate of gas in the reactor varies, thus changing the NH_3 concentration in the catalyst bed, are shown in Fig. 7. The order of the reaction in ammonia was determined from the dependence of the reaction rate on the gas flow rate following the method of Holzman *et al.* (34). The reaction orders determined from these experiments are shown in Table 8 and compared with the results of Nwalor and Goodwin for Ru/SiO_2 (35). The ammonia synthesis reaction was also performed with D_2 instead of H_2 as a reactant. As shown in Fig. 8, no isotope effect was observed.

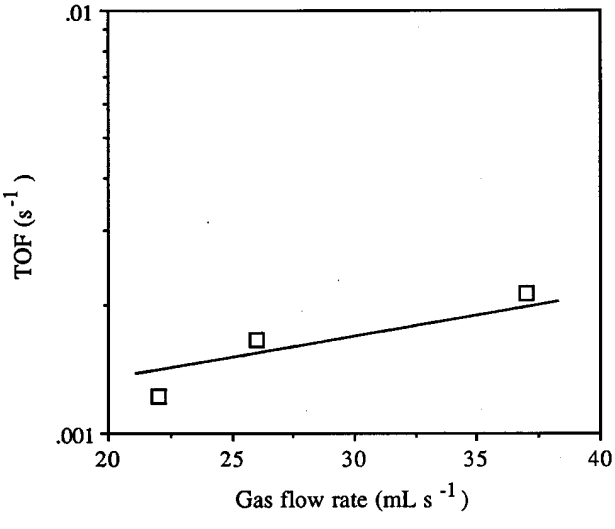

FIG. 7. Dependence of the ammonia synthesis rate at 623 K on the gas recirculation rate.

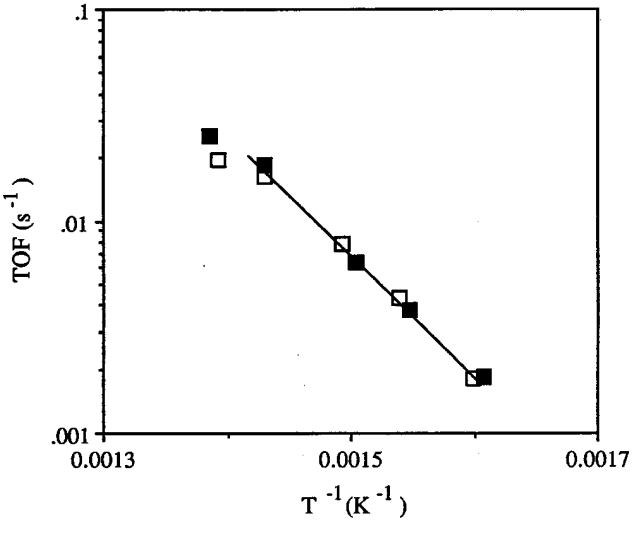

FIG. 8. Comparison of rates of ammonia synthesis with H_2 (open squares) and D_2 (filled squares) over Ru/BaX.

DISCUSSION

The partial oxygen charges of the zeolites used in this work, calculated from the intermediate Sanderson electronegativities of the elements, are shown in Table 9. Although the relationship between the partial oxygen charge and ammonia synthesis rate proposed by Cisneros and Lunsford (22, 23) holds for alkali-exchanged zeolite X, the alkaline-earth-exchanged zeolites do not conform to this model. The most active catalyst, Ru/BaX, had a greater electronegativity and a less negative partial oxygen charge than even Ru/KX. Thus, the effectiveness of the promoters is clearly affected by factors other than the overall electronegativity of the support. One possible suggestion is that the excess alkali present in the samples (see Table 1) is responsible for the increase in activity.

Another plausible explanation for the greater ammonia synthesis rates over alkaline-earth-exchanged Ru/X, compared to alkali-exchanged Ru/X, could be differing degrees of pore blockage. For example, although both Ba^{+2} and K^{+} have similar ionic radii, half as much Ba^{+2} as K^{+} is required for charge balance of the zeolite framework. Promoter ions could be blocking sites on the ruthenium clusters, and such an effect would presumably be more severe in Ru/KX than Ru/BaX. Therefore, the intrinsic rates for NH_3 synthesis over Ru/KX could be greater than that of Ru/BaX, as predicted on the basis of the zeolite electronegativity, but appear to be less due to the effects of partial pore blockage. A proper comparison to determine if such pore blockage is a problem cannot be made using pore volumes calculated on a per gram of catalyst basis (such as those in Table 4), due to the large differences in the atomic weights of the promoter ions. Instead the pore volumes were recalculated on a per mole of unit cells basis, as shown in Table 10. On this basis, the pore volume of Ru/BaX is within 5% the value for Ru/KX. Blockage by ions within the zeolites may not be responsible for the differences in catalyst reactivity, but the effect of pore volume cannot be completely ruled out at this time.

The reason for the unexpected promotional effect of barium on catalysis by supported ruthenium is unclear at this time. From preliminary IR studies in our laboratory, the stretching frequency of linearly adsorbed NO was the same for Ru/CsX and Ru/BaX (36). Therefore, promotion of ammonia synthesis by electron donation to the supported Ru cluster is unlikely. Recent N_2 TPD studies of Ru/MgO suggest that only a small fraction of the Ru surface is highly active for ammonia synthesis (37). A possible role of the promoter may be restructuring the Ru cluster to expose a greater proportion of these highly active sites.

TABLE 9

Partial Oxygen Charges of Zeolite X Catalysts

Catalyst	S_{int}[a]	δO[b]
Ru/KX	3.22	−0.42
Ru/CsX	3.16	−0.43
Ru/CaX	3.55	−0.35
Ru/BaX	3.54	−0.35
Ru/BaX (II)	3.63	−0.33

[a] Intermediate Sanderson electronegativity.
[b] Partial oxygen charge.

TABLE 10

Micropore Volumes for Ru Supported on Zeolite X

Catalyst	Micropore volume (cm^3 (mol unit cells)$^{-1}$)
Ru/KX	3320
Ru/CsX	2574
Ru/CaX	2832
Ru/BaX	3449

The differences in apparent activation energies and turnover frequencies for magnesia-supported Ru catalysts in this study and in the work of Aika *et al*. are probably due to differences in Ru precursors and in the source of the magnesia supports. Aika *et al*. added promoters in the form of nitrates. Decomposition of the nitrates was performed in flowing H_2, and occurred at the same time as reduction of ruthenium (11). In contrast, in this work, ruthenium was reduced to the metal before promoters were added, the promoters were added as acetates, and the acetates were decomposed by heating in flowing N_2. In addition, the support in this study was a high-surface-area magnesia (100 $m^2\ g^{-1}$ before addition of Ru and promoters (38), while the magnesia used by Aika *et al*. had a surface area of 16 $m^2\ g^{-1}$ (11).

The kinetics of the ammonia synthesis reaction over Ru appear to be different than for Fe. Over iron-based catalysts at typical experimental conditions, the forward rate expression can be approximated as

$$r = k'[N_2]\{[H_2]^3/[NH_3]^2\}^n, \quad [1]$$

with $0 < n < 1$ (39, 40). For the ruthenium catalysts in Table 8, the reaction order in N_2 remains approximately 1, the order in NH_3 remains negative, but the order in H_2 becomes negative.

Over iron catalysts, the rate-determining step has been found to be the dissociative adsorption of N_2 (39, 41–45). To investigate the rate-determining step for the catalysts in this work, ammonia was synthesized using deuterium as a reactant. No D_2 isotope effect was observed. Aika and Ozaki also found no change in the reaction rates using D_2 instead of H_2 (46). This lack of an isotope effect indicates that the rate-determining step does not involve a surface species that contains hydrogen (46), such as

$NH_{2_{ads}}$, so that the dissociation of N_2 most likely remains the rate-determining step.

An explanation for the negative order of reaction in H_2 involves an increase in the steady state surface coverage of hydrogen atoms. The most abundant reactive intermediate (mari) for ammonia synthesis over iron is believed to be N^*, atomic nitrogen on a surface site (39). However, Urabe *et al*. studied the effect of H_2 on the isotopic equilibration of N_2 on various ruthenium catalysts and found that most adsorption sites on Ru were occupied by hydrogen atoms (47). The fraction of adsorption sites occupied by nitrogen atoms was not negligible, as the ratio of H^* to N^* was approximately 5 (47). Modeling the forward reaction using dissociative adsorption of N_2 as the rate-determining step and H^* and N^* as the most abundant reactive intermediates gives the following sequence of steps,

$$\text{Step 1:}\quad N_2 + 2^* \longrightarrow 2N^*$$
$$\text{Step 2:}\quad H_2 + 2^* \rightleftharpoons 2H^*$$
$$\text{Step 3:}\quad N^* + 3H^* \rightleftharpoons NH_3 + 4^*,$$

where step 1 is the rate-determining step, and step 2 is in quasi-equilibrium. Because the mari's are produced by steps 1 and 2, all other equilibrated nonelementary steps may be summed up into an overall equilibrated reaction (39), step 3. The overall rate is the same as that of the rate-determining step, so that

$$r = r_1 = k_1[N_2][^{**}], \qquad [2]$$

where $[^{**}]$ represents the number density of empty pairs of adjacent surface sites (39). Since $[^{**}]$ is proportional to $[^*]^2[L]^{-1}$, where $[L]$ is the number density of sites on the catalyst, the rate of step 1 can also be written as

$$r = r_1 = k_1'[N_2][^*]^2[L]^{-1}. \qquad [2a]$$

The number density of sites is equal to the sum of the concentrations of unoccupied sites and sites covered by the mari's:

$$L = [^*] + [H^*] + [N^*]. \qquad [3]$$

From equilibrium,

$$K_2 = [^*]^2[H_2]/[H^*]^2 \qquad [4]$$

and

$$K_3 = [N^*][H^*]^3/[NH_3][^*]^4. \qquad [5]$$

Solving Eqs. [3], [4], and [5] for $[^*]$ yields

$$[^*] = [L]/\left\{1 + [H_2]^{1/2}/K_2^{1/2} + K_3K_2^{3/2}[NH_3]/[H_2]^{3/2}\right\}. \qquad [6]$$

Substituting for $[^*]$ in Eq. [2a] gives the following rate expression:

$$r = k_1'[L][N_2]/\left\{1 + [H_2]^{1/2}/K_2^{1/2} + K_3K_2^{3/2}[NH_3]/[H_2]^{3/2}\right\}^2. \qquad [7]$$

The overall rate order in dihydrogen from this equation could appear to be either positive or negative depending on which of the two terms in the denominator that contains $[H_2]$ dominates. Indeed, Aika *et al*. found that the reaction order in H_2 was positive for ammonia synthesis over Ru/Al_2O_3 and Ru/MgO, but became negative over $Ru/Cs–Al_2O_3$ and Ru/Cs–MgO (48). Also, as shown in Table 8, as the order in H_2 becomes more negative, the order in NH_3 approaches zero, which is the behavior expected from Eq. [7] when the second term of the denominator ($[H_2]^{1/2}/K_2^{1/2}$) dominates over the third term ($K_3K_2^{3/2}[NH_3]/[H_2]^{3/2}$).

Stoltze and Nørskov have used a microscopic model to evaluate the kinetics of ammonia synthesis on iron catalysts at vanishingly small conversion levels (49). They predict that the reaction will be inhibited by dihydrogen and zero order in ammonia under conditions of low ammonia partial pressures, which is consistent with the results presented here for supported ruthenium catalysts.

CONCLUSIONS

On zeolite X, ruthenium exists as small particles, 1.0–1.3 nm in diameter, as determined by H_2 chemisorption. Clusters of a similar size can also be synthesized on MgO, but larger clusters are formed on MCM-41 molecular sieves. Through careful synthesis to maximize the amount of cesium incorporated, a Ru/CsX catalyst can be made that is more active for ammonia synthesis than Ru/KX. Calculations based on elemental analysis confirmed that the CsX support in this study was less electronegative than KX. Turnover frequencies over Ru/KX increased with the metal cluster size, confirming the structure sensitivity of ammonia synthesis over ruthenium. A comparison of the reaction rates over ruthenium using zeolite X and MCM-41 as supports suggests that the microporosity of zeolite X is not a controlling factor limiting the rate of ammonia synthesis.

Unexpectedly, alkaline-earth metals were found to be more effective promoters than alkali metals for Ru supported on zeolite X and MCM-41. For example, at 623 K, turnover frequencies were more than three times as great over Ru/BaX than over Ru/CsX. The Ru/BaX and Ru/KX catalysts had nearly identical pore volumes, as measured by dinitrogen adsorption, suggesting that pore blockage by ions within the zeolites does not account for the differences in reaction rates.

The kinetics of ammonia synthesis were considerably different over ruthenium than what has been reported for industrial iron catalysts. The reaction order in H_2 is positive over Fe, but was negative over Ru in this study. Dinitrogen adsorption is generally believed to be the rate determining step in ammonia synthesis of iron. Since the reaction over Ru remained first order in N_2 and no deuterium isotope effect was observed, dissociation of N_2 is also likely to

be the rate-determining step on Ru. We therefore propose that the negative reaction order in dihydrogen results from adsorbed hydrogen atoms covering a significant fraction of the active Ru surface.

ACKNOWLEDGMENTS

This work was supported by U.S. National Science Foundation Young Investigator Award CTS-9257306 and the Dow Chemical Company. We thank Mr. Andrew Q. Campbell from Dow Chemical Co. for synthesizing some of the catalyst samples.

REFERENCES

1. Kaufman, G., *Today's Chemist.* Aug., 10 (1990).
2. Ozaki, A., Aika, K., Furuta, A., and Okagami, A., US patent 3,770,658 (1973).
3. Aika, K., Hori, H., and Ozaki, A., *J. Catal.* **27**, 424 (1972).
4. Menon, P. G., *Appl. Catal. A* **93**, N16 (1993).
5. Goethel, P.J., and Yang, R. T., *J. Catal.* **111**, 220 (1988).
6. Baker, R. T. K., *Carbon* **24**, 715 (1986).
7. Ozaki, A., and Aika, K., *in* "Catalysis: Science and Technology" (J. R. Anderson and M. Boudart, Eds.), Vol. 1, p. 87. Springer-Verlag, Berlin, 1981.
8. Aika, K., Ohya, A., Ozaki, A., Inoue, Y., and Yasmuri, I., *J. Catal.* **92**, 305 (1985).
9. Murata, S., and Aika, K., *J. Catal.* **136**, 110 (1992).
10. Murata, S., and Aika, K., *J. Catal.* **136**, 118 (1992).
11. Aika, K., Takano, T., and Murata, S., *J. Catal.* **136**, 126 (1992).
12. Murata, S., and Aika, K., *Appl. Catal. A* **82**, 1 (1992).
13. Lee, G. v. d., and Ponec, V., *Catal Rev.—Sci. Eng.* **29**, 183 (1987).
14. Smith, J. R., Arlinghaus, F. J., and Gay, J. G., *Phys. Rev. B* **26**, 1071 (1982).
15. Lang, N. D., Holloway, S., and Nørskov, J. K., *Surf. Sci.* **150**, 24 (1985).
16. Over, H., Bludau, H., Skottke-Klein, M., Moritz, W., and Ertl, G., *Phys. Rev. B* **46**, 4360 (1992).
17. Uner, D. O., Pruski, M., Gerstein, B. C., and King, T. S., *J. Catal.* **114**, 530 (1994).
18. Strongin, D. R., and Somorjai, G. A., *J. Catal.* **109**, 51 (1988).
19. Strongin, D. R., and Somorjai, G. A., *Catal. Lett.* **1**, 61 (1988).
20. Benndorf, C., and Madey, T. E., *Chem. Phys. Lett.* **101**, 59 (1983).
21. Gallezot, P., *Catal. Rev. Sci. Eng.* **20**, 121 (1979).
22. Cisneros, M. D., and Lunsford, J. H., *J. Catal.* **141**, 191 (1993).
23. Cisneros, M. D., Ph.D. dissertation, Texas A&M University, December, 1990.
24. Aika, K., Shimazaki, K., Hattori, Y., Ohya, A., Ohshima, S., Shirota, K., and Ozaki, A., *J. Catal.* **92**, 296 (1985).
25. Oukaci, R., Sayari, A., and Goodwin, J. G., Jr., *J. Catal.* **106**, 318 (1985).
26. Beck, J. S., Vartuli, J. C., Roth, W. J., Leonowicz, M. E., Kresge, C. T., Schmitt, K. D., Chu, C. T.-W., Olson, D. H., Sheppard, E. W., McCullen, S. B., Higgins, J. B., and Schlenker, J. L., *J. Am. Chem Soc.* **114**, 10834 (1992).
27. Crumbaugh, G., M.S. Thesis, University of Virginia, May 1995.
28. Sherry, H. S., *J. Phys. Chem.* **70**, 1158 (1966).
29. Barrer, R. M., Rees, L. V. C., and Shamsuzzoha, M., *J. Inorg. Nucl. Chem.* **28**, 629 (1966).
30. Kotz, J. C., and Purcell, K. F., "Chemistry and Chemical Reactivity." Saunders, Philadelphia, 1987.
31. Hathaway, P. E., and Davis, M. E., *J. Catal.* **116**, 263 (1989).
32. Lippens, B. C., and deBoer, J. H., *J. Catal.* **4**, 319 (1965).
33. Aika, K., Kawahara, T., Murata, S., and Onishi, T., *Bull. Chem. Soc. Jpn.* **63**, 1221 (1990).
34. Holzman, P. R., Shiflett, W. K., and Dumesic, J. A., *J. Catal.* **62**, 167 (1980).
35. Nwalor, J. U., and Goodwin, J. G., *Top. Catal.* **1**, 285 (1994).
36. Fishel, C. T., Ph.D. dissertation, University of Virginia, May 1996.
37. Rosowski, F., Hinrichsen, O., Muhler, M., and Ertl, G., *Catal. Lett.* **36**, 229 (1996).
38. McKenzie, A. L., Fishel, C. T., and Davis, R. J., *J. Catal.* **138**, 547 (1992).
39. Boudart, M., and Djega-Mariadassou, G., "Kinetics of Heterogenous Catalytic Reactions." Princeton Univ. Press, Princeton, NJ, 1984.
40. Temkin, M. I., and Pyzhev, V., *Acta Phyicochim. USSR* **12**, 327 (1940).
41. Emmett, P. H., *in* "The Physical Basis for Heterogenous Catalysis." (E. Dragoulis and R. I. Jaffee, Eds.), p. 3, Plenum, New York, 1973.
42. Emmett, P. H., and Brunauer, S., *J. Am. Chem. Soc.* **56**, 35 (1934).
43. Ozaki, A., Taylor, H., and Boudart, M., *Proc. Royal Sco. London A.* **258**, 47 (1960).
44. Aika, K., and Ozaki, A., *J. Catal.* **13**, 232 (1969).
45. Morikawa, Y., and Ozaki, A., *J. Catal.* **23**, 97 (1971).
46. Aika, K., and Ozaki, A., *J. Catal.* **16**, 97 (1970).
47. Urabe, K., Aika, K., and Ozaki, A., *J. Catal.* **42**, 197 (1976).
48. Aika, K., Kumasaka, M., Oma, T., Kato, O., Matsuda, H., Watanabe, N., Yamazaki, K., Ozaki, A., and Onishi, T., *Appl. Catal.* **28**, 57 (1986).
49. Stoltze, P., and Nørskov, J. K., *J. Catal.* **110**, 1 (1988).